

Studies and tests on slender plate girders without stiffeners shear strength and local web crippling

Autor(en): **Bergfelt, Allan**

Objektyp: **Article**

Zeitschrift: **IABSE reports of the working commissions = Rapports des commissions de travail AIPC = IVBH Berichte der Arbeitskommissionen**

Band (Jahr): **11 (1971)**

PDF erstellt am: **14.08.2024**

Persistenter Link: <https://doi.org/10.5169/seals-12053>

Nutzungsbedingungen

Die ETH-Bibliothek ist Anbieterin der digitalisierten Zeitschriften. Sie besitzt keine Urheberrechte an den Inhalten der Zeitschriften. Die Rechte liegen in der Regel bei den Herausgebern.

Die auf der Plattform e-periodica veröffentlichten Dokumente stehen für nicht-kommerzielle Zwecke in Lehre und Forschung sowie für die private Nutzung frei zur Verfügung. Einzelne Dateien oder Ausdrucke aus diesem Angebot können zusammen mit diesen Nutzungsbedingungen und den korrekten Herkunftsbezeichnungen weitergegeben werden.

Das Veröffentlichen von Bildern in Print- und Online-Publikationen ist nur mit vorheriger Genehmigung der Rechteinhaber erlaubt. Die systematische Speicherung von Teilen des elektronischen Angebots auf anderen Servern bedarf ebenfalls des schriftlichen Einverständnisses der Rechteinhaber.

Haftungsausschluss

Alle Angaben erfolgen ohne Gewähr für Vollständigkeit oder Richtigkeit. Es wird keine Haftung übernommen für Schäden durch die Verwendung von Informationen aus diesem Online-Angebot oder durch das Fehlen von Informationen. Dies gilt auch für Inhalte Dritter, die über dieses Angebot zugänglich sind.

Studies and Tests on Slender Plate Girders without Stiffeners Shear Strength and Local Web Crippling

Etudes et essais sur les poutres à âme mince sans raidisseurs
Résistance au cisaillement et voilement de l'âme sous charges
concentrées

Untersuchungen und Versuche an dünnwandigen Blechträgern
Schubfestigkeit und Stehblechbeulen unter Einzellasten

ALLAN BERGFELT

Professor

Chalmers University of Technology
Göteborg, Sweden

I. Shear test results

Summary of theories

For girders with normal web imperfections the theoretical computation of linear elastic instability does not give the real bearing capacity. For plate girders with web stiffeners better results are obtained with Wagner's [1] theory of tension fields as adjusted by Basler and Thürlimann [2] and still better as improved by Rockey and Skaloud [3].

These theories are not applicable to girders without web stiffeners or with stiffeners only at the supports. For such girders the use of Karman's [4] equation of finite plate theory gives better results. An early approximate solution to this equation was given by Bergman [5]. During the long period of time after the publication of this paper not more than a few tests on very slender girders with end stiffeners only have been reported.

Test results on girders without intermediate web stiffeners

Unpublished reports on test results have been given by C.A. Granholm 1960-62 [6, 7] and a summary has been published [8]. Further results are included in tests published by Bergfelt and Hövik [9].

The results obtained in these tests are plotted in the diagrams fig. 3 and 4 (filled dots). In both diagrams comparison curves computed according to Bergman's theory [5] are shown. In fig. 3 the directly computed mean τ -values are marked [10] but in fig. 4 these values are reduced in order to correspond to an infinite long girder with a yield stress $\sigma_Y = 2200 \text{ kp/cm}^2$, which yield stress was Bergman's base value.

As a further comparison also some values from tests on slender girders with web stiffeners are marked ($\alpha = a/h > 2$ and $h/d > 150$). Even some tests with h/d equal to 100, 120 and 140 are included. This is motivated because in these particular

cases σ_Y in the web (3800 kp/cm^2) or in the flanges (5600 kp/cm^2) was very high [11] resp. [12] and these girders therefore might show a different behaviour [11]. The characteristic values for the test are recorded in Table 1.

The comparison curves in fig. 3 and the characteristic curve in fig. 4 are based on the diagrams numbered VII 2 and VII 3 in reference [5]. These diagrams are here given in a somewhat revised form as fig. 1 and fig. 2.

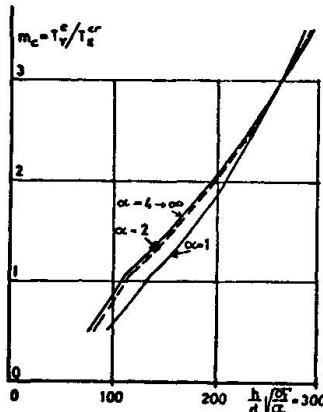


Fig. 1 Collapse shear force at web yield stress σ_Y divided by critical shear force at ideal buckling, $m_c = T_c^C/T_c^E$ as function of slenderness ratios h/d made comparable by multiplying with $\sqrt{\sigma_Y/\sigma_0}$. Here σ_0 is chosen to 2200 kp/cm^2 . Aspect ratios one and upwards. [5]

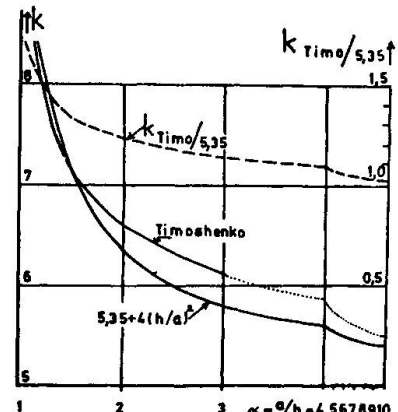


Fig. 2 Diagram over buckling coefficient k in $\tau^{CR} = k \pi^2 D / dh^2$ for different aspect ratios α of plates with hinged edges. Values calculated by S Timoshenko and the approximate curve $5.35 + 4 (h/a)^2$. [5] The right vertical scale measures the factor $k_{\text{Timoshenko}}/5.35$.

Ref.	No	h/d	α	σ_Y	l	$b \cdot t$	$h \cdot d$	σ	τ	$\frac{h}{d} \sqrt{\frac{\sigma_Y}{2200}}$	m_c	$m_{c\sigma}$	k_α/k	τ_{corr}
[9] Bergfelt -Hövik	1:1	300	12	>2600	7,3	175 · 6	600 · 2	1640	467	>325	3,60	4,13	1,02	400
	2:2	300	2,4	(2600)	7,3	175 · 6	600 · 2	2220	635	(325)	3,62	4,16	1,18	470
	3:1	197	17	>2600	9,8	200 · 8	590 · 3	2750	587	>215	2,04	2,25	1,01	525
	3:5	"	"	"	"	"	"	1865	620	"	"	"	"	554
	3:6	"	"	"	"	"	"	940	650	"	"	"	"	580
[5] Bergman	A2	286	2,0	2820		300 · 30	1000 · 3,5	-	655	324	3,42	4,20	1,23	437
	A6	218	3,4	2280		300 · 20	700 · 3,2	-	675	221	2,28	2,30	1,12	595
	A5	175	3,4	3030		300 · 20	700 · 4,0	-	870	206	1,75	2,16	1,12	630
[6] Granholm	E53	270	3,4(1,7)	2800	4,0	130 · 5,4	590 · 2,2	2290	470	305	3,12	3,7	1,12	353
	E54	"	3,4(1,7)	"	4,0	"	"	2350	480	"	"	"	"	362
	C	195	<7	2800	5,9	"	780 · 4	2820	757	220	2,00	2,35	1,04	621
	E32	187	13,4	2800	8,0	180 · 9	596 · 3,1	2240	712	210	1,92	2,21	1,02	607
	E33	"	13,4	"	8,0	"	"	2320	735	"	"	"	"	627
	E42	187	3,4	2800	8,0	200 · 10	600 · 3,1	2440	900	210	1,90	2,18	1,12	700
[2] Basler- Thürlim.	G8-T1	254	3,0	2700					612	281	2,84	3,31	1,14	461
	E1-T1	131	3,0	2940					1012	151	1,25	1,46	1,14	760
[11] Nishino- Okumura	G7	119	2,6	3800	6,0	282 · 22	1080 · 9,1	1300	156	1,10	1,50	1,17	815	
	G8	121	2,6	3800	"	221 · 22	1080 · 9,1	1150	159	1,12	1,54	1,17	715	
	G5	100	2,6	3800	5,5	291 · 22	899 · 9,0	1510	131	0,84	1,22	1,17	890	
	G6	101	2,6	3800	"	212 · 22	900 · 8,9	1320	133	0,85	1,24	1,17	775	
[12] Carskad.	C-AC2	143	5,5	2150	5,8	94 · 9,7	454 · 3,2	5600	845	141	1,39	1,37	1,06	810

Table 1

The test results for long girders with end stiffeners only are all lying close to the characteristic curve in fig. 4. This fact applies to the measuring values E 32, E 33 in ref. [6] as well as the values 1:1, 3:1, 3:5, 3:6 in ref. [9] marked with filled dots, compare Table 1. Some of these test results are based not only on pure shear and bending of the web, but also local web crippling under a point load and flange buckling are acting in a composite way. When σ increased from 940 to 2750 kp/cm^2 τ reduced 10 % [9].

Decimal points are marked with commas, e.g. 1,234 and 0,234 instead of 1.234 and .234. Multiplication is generally marked with a point · but in case there can be risk for mistakes the sign x is used.

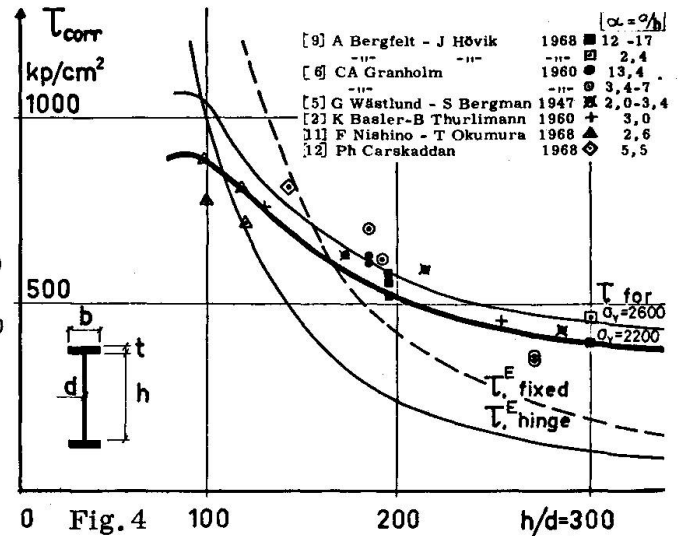
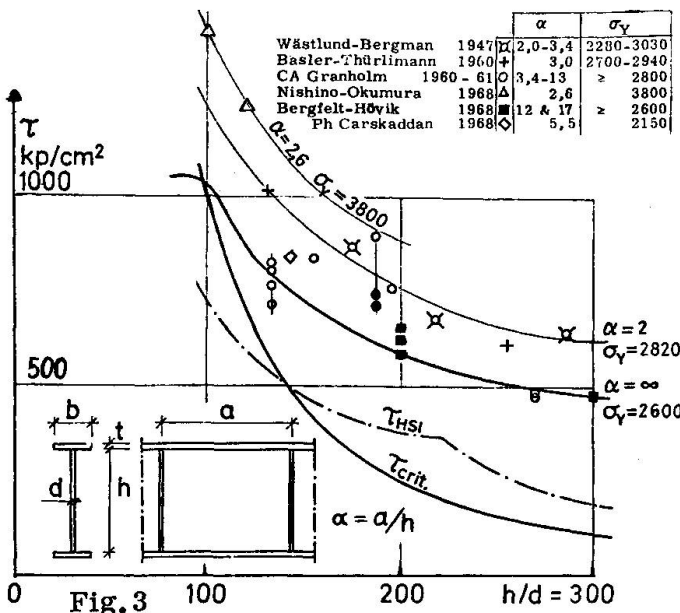


Fig. 3
Nominal shear stresses as function of the web slenderness ratio h/d . Measured test values for ultimate bearing capacity compared with $\tau_{critical}$ for elastic buckling, with allowable stresses according to provisional Swedish specifications (HSI) and with yield stresses computed according to Bergman [Ref. 2 fig. VII 2].
(The figure is copied from [10].)

Fig. 4
Nominal shear stresses as function of the web slenderness ratio h/d . The points computed from the test values for ultimate bearing capacity, see Table 1, are compared with Bergman's characteristic curve for $\sigma_{Y,web} = 2200 \text{ kp/cm}^2$. Comparison also between characteristic curve for $\sigma_{Y,web} = 2600$ and curves of elastic buckling with a hinged web (E_{hinge}) and a restrained web (E_{fixed}).

$$1000 \text{ kp/cm}^2 \text{ (kiloponds/sq. cm)} = 1 \text{ Mp/cm}^2 = 1 \text{ ton/cm}^2 = 14,2 \text{ ksi (kilopounds/sq. in)} \approx 100 \text{ MN/m}^2 \text{ (Mega Newton/sq. m)} = 100 \text{ N/mm}^2$$

The comparison results for girders with lower α -values are also lying relatively close. This might be a mere chance as the flange dimensions of the test girders were not exceptional. Most of these test results are a little too high compared to the characteristic curve indicating the neglect of consideration to the influence of flange stiffness, which is large for small α -values. Some of the results are to the contrary under the curve. For these it is pointed out in the reports that the collapse was caused by flange buckling and not by web buckling [11] or that the end stiffeners might have been insufficient [6].

For girders with end stiffeners only the influence of varying flange areas is not very important. For lower values of α the influence of varying flange areas is great as may be seen from the diagrams given by Rockey and Skaloud [3] or the computation method given in [13].

On the diagram in fig. 4 also buckling curves are shown according to linear, small-deflection theory, on the assumption of the web being hinged to the flange ($k=5,35$) and of full restraint ($k=8,98$). To get a better visual picture of the greatest real load in comparison with the linear theory a curve according to Bergman denoted " τ for $\sigma_Y=2600$ " is shown. The yield limits of all test girders except two were greater than 2600 kp/cm^2 .

The real bearing capacity for slender webs, $h/d > 150$, is larger or even far larger than the linear elastic theory should give even in case of the favourable assumption of a fully restrained web. This holds true even for great initial lateral deformations of the web, e.g. $h/100$ or $5 \cdot 10^{-5} h^2/d$ (c.f. test 3:2 in [10] where δ_{init} was $h/50$).

II. Web Crippling

Presentation and earlier tests

Under great concentrated loads attacking on the upper flange of a plate girder it is necessary to stiffen the girder with web stiffeners. In case of small loads such as from closely spaced purlins no stiffeners are usually necessary except at the supports. With increasing web slenderness ratios it may be questioned if intermediate stiffeners are necessary or not.

Normally the demand for stiffeners is controlled by checking the vertical web stress under the load. An approximate method is to consider the load distribution length to be equal to the width of the purlin increased by the thickness of the flange and the height of the fillet welds. Another method is to distribute the load considering the flange as an elastic beam resting on elastic springs [14]. A third method is naturally to compute stresses and strains without any simplified models and taking into account the real shape of the girder. This method gives an increased amount of computing.

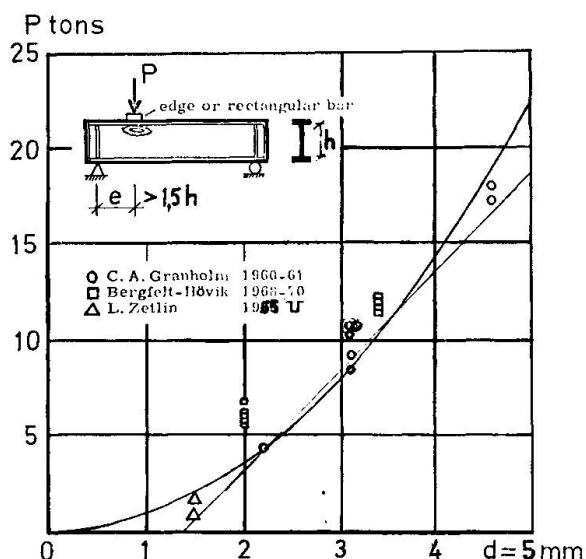


Fig. 5

The dependency of collapse load P on web thickness d , as observed by different authors. (Zetlin's tests were performed on cold-formed Γ -shaped section.)

The figure is copied from [10].

Besides the determination of the vertical web stresses the risk of web buckling has to be investigated. A great many theoretical investigations of this phenomena have been done [e.g. 15, 16]. For girders with slender webs (thickness 2 to 6 mm and h/d varying from 150 to 300) it has been shown [7] that approximate cripple failure loads are given by the simple empirical formula $P = 0,9 d^2$, where P is the cripple load in tons and d is measured in mm. Naturally also the modulus of elasticities and the yield stresses for the flange and web material influence the static behaviour as well as the dimensions of the flanges.

In a paper the author and his co-worker J. Hövik [10] have compared tests done by us with earlier tests and the results are in support of the simplified formula according to [7], see fig. 5. In an earlier paper [9] it is suggested that the dominating importance of the web thickness d over the influence of the flange dimensions may qualitatively be explained by the theory of beam on elastic foundations in taking into account some part of the web in the computation of the stiffness of the "flange beam".

New tests on web crippling in girders without intermediate stiffeners

Despite the accurateness of the empirical curve as demonstrated by the measuring points in fig. 5 the dependency on yield strength and flange dimensions has to be taken

into account in case of deviations from the mean yield strength and in case of varying ratios of flange to web areas.

Therefore a test series has been executed with constant web dimensions 3 x 700 mm and varying flange areas from 6 x 150 mm to 15 x 300 mm.

Under each point load a knife-edge or a plate of width 100 mm was placed to transfer the load. Once the knife-edge was applied first and in the next case the plate. With this procedure the load was not increased to collapse, but the loading was interrupted at successive yielding (if possible). The yield was considered successive when the deformation at a loading stage amounted to at least 0,05 mm during the first five minutes of the stage and when it continued after 15 minutes. During earlier tests [10] this method has been considered satisfactory.

At two points on the girder, D_u and H_u repeated loading cycles were applied. For all loading cycles except one 80% of the static collapse load was used as an upper bound.

The tests are summarized in Table 2 and dimensions in Table 3. Here the values of the yield strength in tension and the results of plate bending tests of the flange material are also given. For the flanges the plate bending tests are converted into the moment at first yield and into the fully plastic moment.

Point	Span m	Flange plate materials				Knife-edge load			10 cm bar load			δ_{init} mm	Strain €	
		Nominal dim. mm	σ_Y kp/cm ²	M_Y cm·kp	M_{pl} cm·kp	Def. No mm	P tons	Def. No mm	P tons					
B	2,4	6 x 150	3 540	3 090	4 990	2	0,8	9,7 ^c	1	0,7	10,8	4,4	€	
B _A	1,4					1	1,6	9,7	-	-	-	0,7		
C	2,4	8 x 200	2 400	5 830	8 450	1	0,8	11,2	2	0,9	12,4	4,5		
F	2,4			5 730	8 290	2	1,3	10,3	1	0,8	10,3	9,5		
C _E	2,4	10 x 250	2 480	14 700	16 000	2	0,9	12,3	1	0,4	13,7	5,2		
G _E	2,4			14 600	15 800	1	0,5	12,3	2	0,8	13,4	4,8		
D	2,4	12 x 250	2 370	23 500	30 100	2	1,0	11,9	1	0,6	10,1	7,0		
G	2,4			23 400	29 900	1	0,6	13,8	2	0,8	14,2	3,6		
E	2,4	15 x 300	3 110	43 300	58 400	2	0,8	15,6 ^c	1	0,7	15,8	4,5		
H	2,4			43 400	58 500	1	0,9	15,4 ^c	-	-	-	-		
H	2,4					1	1,3	15,3	2	1,7	16,1	3,1	€	
B _u	9,4	10 x 250	2 480	14 500	15 700	2	2,3	12,0	1	2,1	13,1	7,7		
E _u	9,4			14 600	15 800	1	0,4	10,4	2	0,5	12,0	10,5	€	
H _u	2,4	10 x 250	2 480	14 800	16 000	1	(0,7)	(9,8)	2	(1,7)	(10,9)	2,4	€	
D _u	9,4			14 700	16 000	1	(1,7)	(9,2) [*]	2	(1,9)	(10,0)	0,8	€	
Web		3 x 700	3 320	78,9	89,3	M_Y and M_{pl} for web in kpcm/cm								

c = collapse, local straightening before test

δ_{init} = initial lateral deformations

€ = strain measurements

() = load applied in 100 loading cycles (each cycle 11 min) and deflection for these loads.

* = for this loading case also 100 loading cycles to 10,2 tons (90% of the static collapse load) were made. The deflection increased from 2,60 mm in the first cycle to 2,71 mm in the last cycle.

Table 2

In the neighbourhood of each load transfer the vertical deformation of the loaded flange was measured as the displacement in relation to the other flange (in 1/1000 mm), see fig. 8. The lateral deflections of the web were also measured.

The vertical deflection of the upper flange in relation to the lower flange, centrally under the point of load attack and corresponding to $3/4 P$ is given in Table 2. For repeated loads corresponding to (P) . This proportion of the final collapse load P was chosen because the deformation increased uniformly up to this stage. Beyond this stage the increase was discontinuous owing to yield and snap buckling (fig. 10).

In some tests the strains were measured by electric strain gages. Here at most 68 gages were used, some of them united in rosettes. Every measuring point was double, symmetrically placed on each side of the web, fig. 9. The readings were collected with recorders.

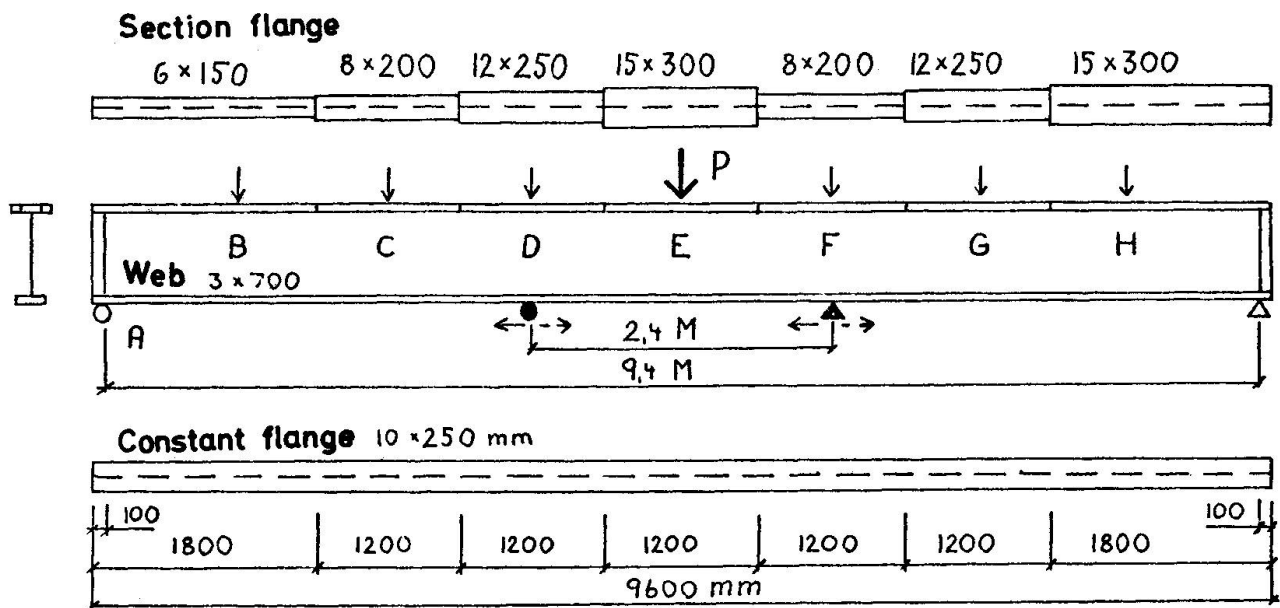


Fig. 6 Test girder

The tests were done on a girder with one flange of dimension 10 x 250 mm and the other flange welded together of sections 6 x 150, 8 x 200, 12 x 250 and 15 x 300 mm. The sections were 1,2 m long and the end sections 1,8 m. The loads were transmitted through various points on the flange of constant cross section and through the midpoints of the sections of the other flange (except in the case of end sections, see fig. 6).

The load was normally introduced by a jack with fixed attachment. In some cases the head of the jack was hinged. In the design of the arrangement of load transmittance the hinge was situated somewhat higher than the upper flange (about 0,1 h). This means that even in the case of a hinged jack the web is somewhat restrained by the flange. During most tests the free span between supports amounted to 2,4 m. Even the ends of the girder were supported.

The point loads have mainly a local influence on the flange, from which follows that the influence of the change in flange area far from the loading point is small as much as the web is continuous. A check of this assumption is obtained by the results from the loading on the flange of constant area, which well accommodate the results on the other flange. That the result even for the thickest flange section 15 x 300 mm, is in detail correct, is not safeguarded.

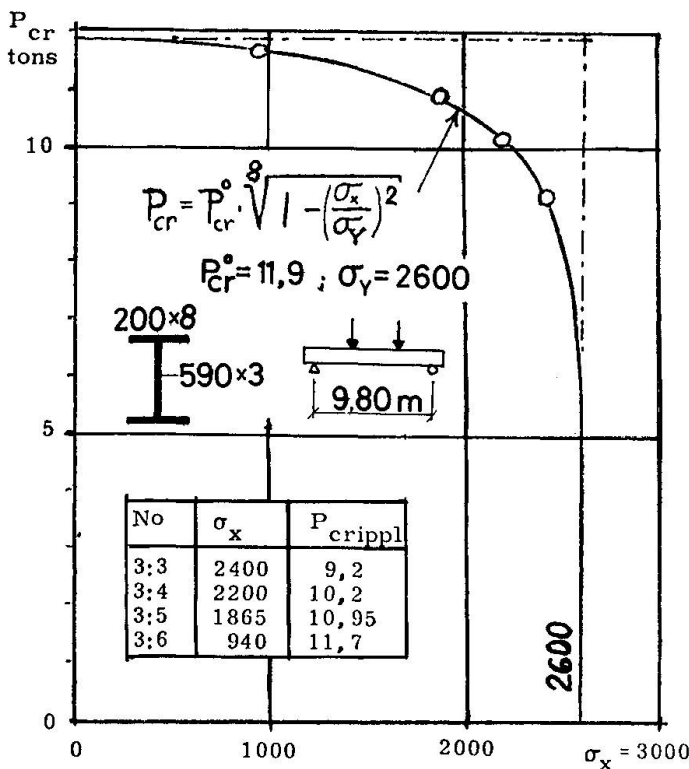


Fig. 7 Interaction formula
 $P_{cr} = P_{cr}^0 [1 - (\sigma/\sigma_Y)^2]^{1/8}$
 from [10] compared with test values from [9].

over the whole length of the girder with an increasing number of measuring points at the points of load attack. The thickness varied between 3,19 and 3,33 mm with the mean value $3,26 \pm 0,04$ mm.

The initial shape of the girder was measured under each point of load attack before loading. Because of residual deformations after previous loadings etc. the initial position in some cases changed somewhat. The greatest initial lateral deflections are given in Table 2. The lateral deflections during the test were measured by a recording gauge (0,001 mm) placed 5 cm under the loaded flange. Several other points were measured from a special vertical reference plane and in case of residual buckles they were levelled in up to 400 points.

Discussion

Introductorily it was stated that the main factors caused by point loads regarded stresses and buckling. The different factors also influence each other and the risk of combined action is probable. Therefore a more complete survey of the different causes may be done as follows.

- A. Web stresses under the points of load attack.
- B. Web buckling under concentrated loads.
- C. Web crippling, defined here as local cripples under a concentrated load, which may develop under high compressive stresses in combined action with bending stresses and local buckling.
- D. The influence of A, B and C on the bearing capacity of the girder.

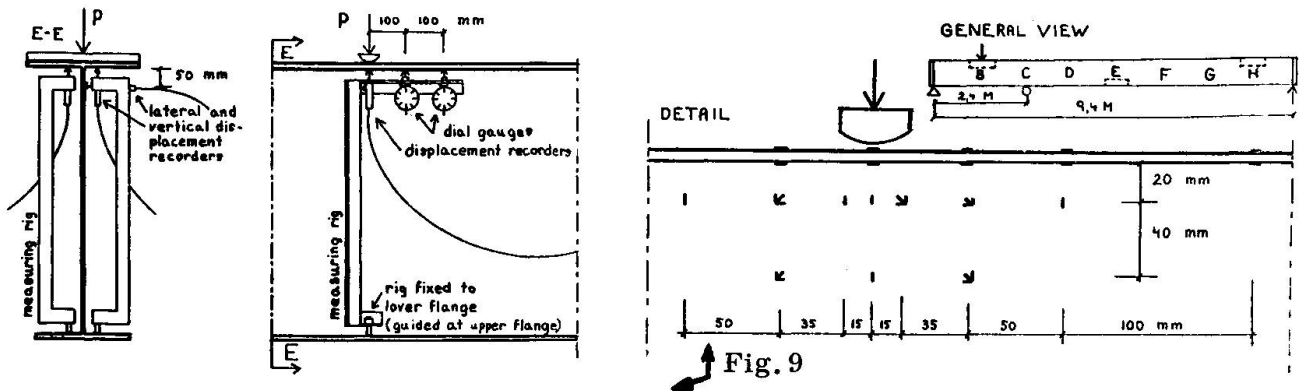
For the chosen span width the compressive bending stresses in the flange during web crippling have amounted to between 200 and 600 kp/cm². (With some correction for the end supports). Earlier investigations show that for so small stresses the bending stress has a very small influence on the cripple load (cf fig. 7). Also the results in ref. [17] illustrate the small interaction, but refer to tests with loading lengths that are longer compared to the beam depth and with a relatively thick web, h/d = 40.

Test results

Certain test results as described above are summarized in Table 2 and 3 as well as in fig.10. Furthermore some results from strain gage measurements for the loading case B:2 are in detail shown in fig.13.

The thickness of the web plate was measured in 220 points distributed

Fig. 8 Dial gauges for vertical displacement of the loaded flange and for lateral deflection at one point of the web.



Electric strain gages for test B. Similar arrangements for tests H and E_u. Strain gages were placed also on the unloaded flange. In test E_u more gages were of rosette type. Under the knife-edge there was a plate of 1,0 mm with recesses for the gages and leads.

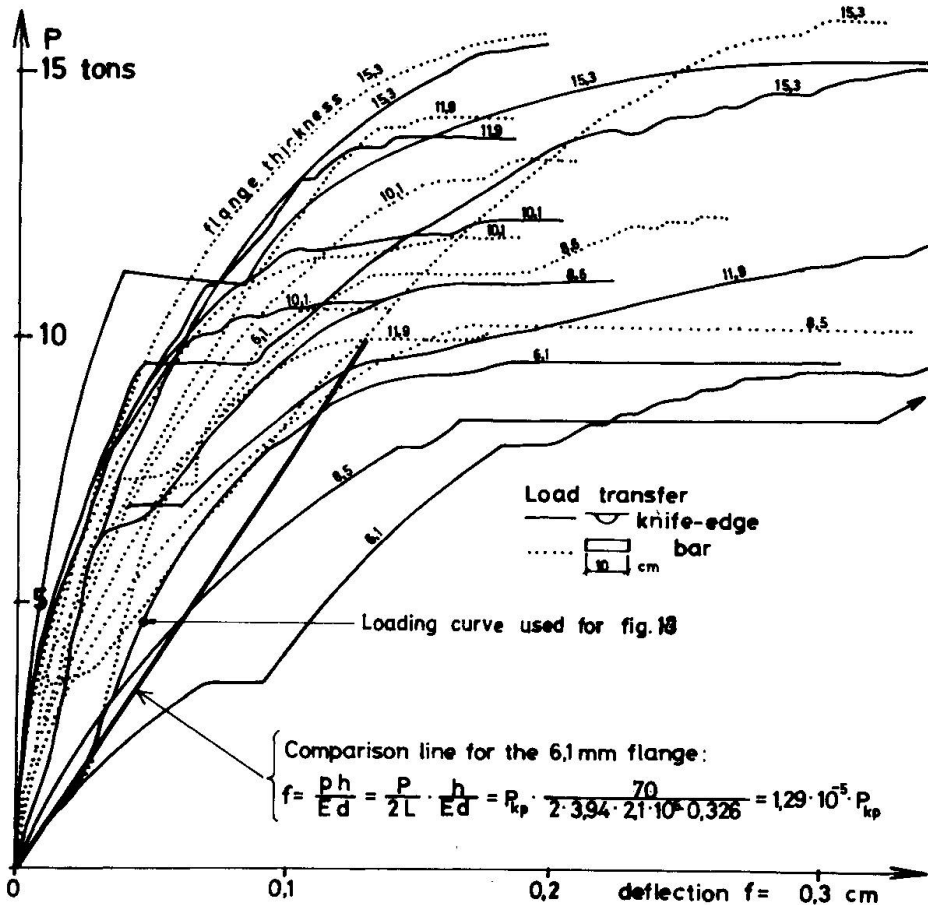


Fig.10 Vertical deflection of the loaded flange directly under the concentrated load

	Flange mm	I _f cm ⁴	L ₀ cm	I _T cm ⁴	e ₀ cm	L _{T0} cm	L _T * cm
B	6,1 x 151	0,284	3,94	29,8	0,98	12,6	26,6
C	8,5 x 200	1,025	5,45	34,3	0,83	13,1	27,7
C	10,1 x 250	2,08	6,50	37,3	0,80	13,3	28,4
D	11,9 x 253	3,56	7,42	41,0	0,85	13,7	29,1
E	15,3 x 302	9,01	9,35	49,7	0,94	14,4	30,6

Table 3
Dimensions and elastic lengths L.

* For δ₀ = h/100 = 7 mm
For δ₀ = h/50, L_T is to be multiplied with 1,4.

A. Compressive web stresses under the point load is a factor that limits the load.

a. - Computing stresses without using a simplified theory is a difficult task for a beam with such a slender web as used here. Even small lateral deflections result in a behaviour that differs very much from case to case. Some guidance may, however, be found in treaties on solid beams as ref. [18]. In this preliminary report of the actual tests only approximate methods are used.

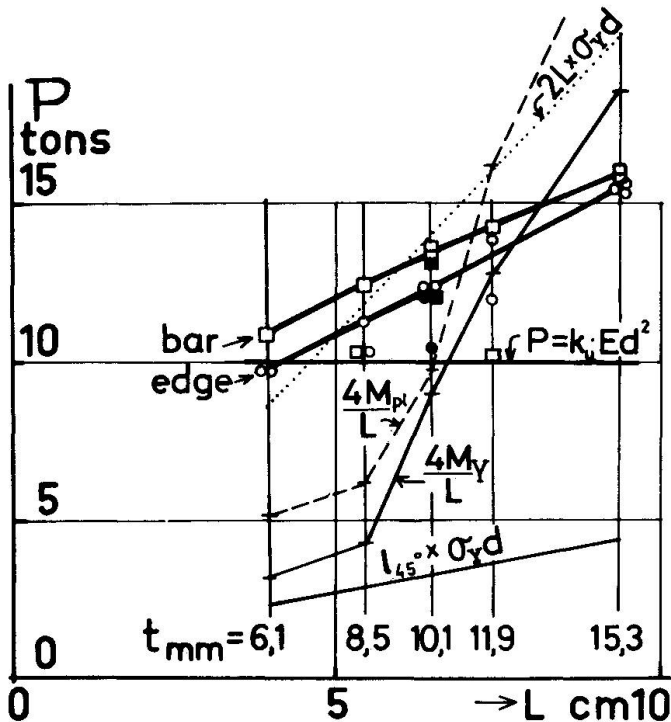


Fig. 11 Measured values of $P_{cripple}$ compared with values calculated under different assumptions. σ_Y , M_Y and M_{pl} from table 2.

b - Assuming a load distribution at an angle of 45° through the flange to the web the load is assumed limited by yield inside this region. The corresponding load is marked on fig. 11. No consideration is taken to combined action. The load calculated in this way $P = \sigma_Y \cdot l_{45^\circ} \cdot d$ is far below the greatest observed load (24 to 28% of it only). Even in case the yield stress is substituted by the compressive strength, the real loads by far surpass the calculated ones.

c. - For a beam on elastic foundations the distribution of the reactions, moments, etc. is given as a function of the "elastic length" L . The application to I-girders is given in [14] and a summary of the different function diagrams of interest is found in an "Appendix" to [10].

Elastic length $L = \sqrt[4]{4EI/Cd}$. Maximum web stress under the point load $\sigma = P/2Ld$. Maximum flange moment $M = PL/4$.

The moment of inertia I used in the computation of the compressive web stress is assumed to be equal to that of the flange plate $I = bt^3/12$. As to the computation of the flange bending stress and the web buckling load this value of the moment of inertia has been used as well as the resulting values when a part ($20 \cdot d$) of the web is supposed to be included thus considering the elastic beam as a T-section^{*)}.

The spring constant C corresponding to the web support of the flange was computed according to two different assumptions. On one hand the web has been assumed to be plane and its lateral deflection has been neglected. On the other hand it has been assumed that the vertical deformation increases^{**)} owing to an initial lateral deflection of the web with pitch $h/100$ (or about $5 \cdot 10^{-5} \cdot h^2/d$), which according to the measurements was a proper value.

On fig. 11 the load corresponding to maximum stress in the web directly under the point load is marked when this stress equals the yield limit e.g. $P = \sigma_Y \cdot 2Ld$. As seen the assumption that the flange plate only is load-distributing gives computed loads almost equal to or greater than the observed ones.

*) and **) see next page.

The flange has to take up the bending moment corresponding to the applied load distribution, however. On fig. 11 the load corresponding to first yield and fully plastic moment is marked, that is $P = 4 M/L$ where M is given in Table 2.

It is seen that the thinner flanges do not have sufficient bending stiffness and thus should not e. g. for the flange dimensions 6 x 150 mm carry more than 3 to 5 tons. Notwithstanding this fact the girder is able to support a maximum load of about 9,7 tons.

The computations of the collapse load illustrated in fig. 12 explains this. At $P = 3$ tons the flange moment under the point load is $M = PL/4 = 3 \cdot 3,94/4 = 2,95$ tons x cm (tcm), shortly under the moment at first yield 3,09 (Table 2), where flow takes place in a small region in the outermost parts of the flange plate. With increasing load a certain strain redistribution takes place, but not until the moment for $P = 5$ tons equals about 4,91 tcm the bearing capacity of the flange is nearly exhausted. The moment then approximately equals the plastic moment 4,99 t according to Table 2. The maximum web stress is $\sigma = P/2 Ld = 5000/2 \cdot 3,94 \cdot 0,326 = 1950$ kp/cm². On fig. 12 these extreme values are marked as well as moment and stress in the neighbourhood of the point of load attack computed according to the "theory of beams on elastic foundations" (from Appendix in [10]).

Above $P = 5$ tons the flange functions as hinged under the point load. For an increase to $P = 7$ tons the flange functions as a hinged beam loaded with 2 tons or as two semiinfinite beams loaded each with a point load of 1 ton at the end. The increment in moment obtains its maximum value $M = 1/2 \times 2 \cdot L \cdot 0,3224 = 1,27$ tcm at a distance $\pi/4 \times L = \pi/4 \times 3,94 = 3,1$ cm from the point load.

The increment in web stress obtains the maximum value $\sigma = 1/2 \times 2000 \cdot 2/3,94 \cdot 0,326 = 1560$ kp/cm². The resulting stress in the critical point is thus $1950 + 1560 =$

*)

Different theories give values from 15 to $40 \cdot d$. From the observed folding deformations and strains in the tested web the value $20 \cdot d$ is chosen here, but of course it ought to be dependent on the dimensions of the flange too.

**)

The compression under load p per unit length is for an initially plane web $f = ph/Ed$ and the spring constant is $Cd = Ed/h$. Considering flange stiffness only L is equal to $L = \sqrt[4]{bt^3/3 \cdot h/d}$.

The initial deflection δ_0 of a hinged strut of length l causes an additional shortening $\Delta f = p \cdot \delta_0^2 \cdot l/2 EI$ due to small increase in lateral deflections. The measurements of the initial web deflections and an evaluation of flange restraint have motivated that the web as to bending may be considered as a plate hinged at two edges at a distance $0,7 h$ apart. The total web shortening in the case of initial deformations therefore is

$$f_{\text{tot}} = f + \Delta f = \frac{ph}{Ed} (1 + 4,2 \cdot \delta_0^2/d^2)$$

The spring constant is correspondingly diminished.

The load distribution is over a short length only. This implies that the computation as to the web behaviour as single-acting springs gives rise to great errors due to shear and plate action.

= 3570 kp/cm² and therefore it is only locally somewhat over the yield stress $\sigma_Y = 3320$ kp/cm² according to the fig. For further increments of load the web pressure can not increase in the region where σ_Y is surpassed.

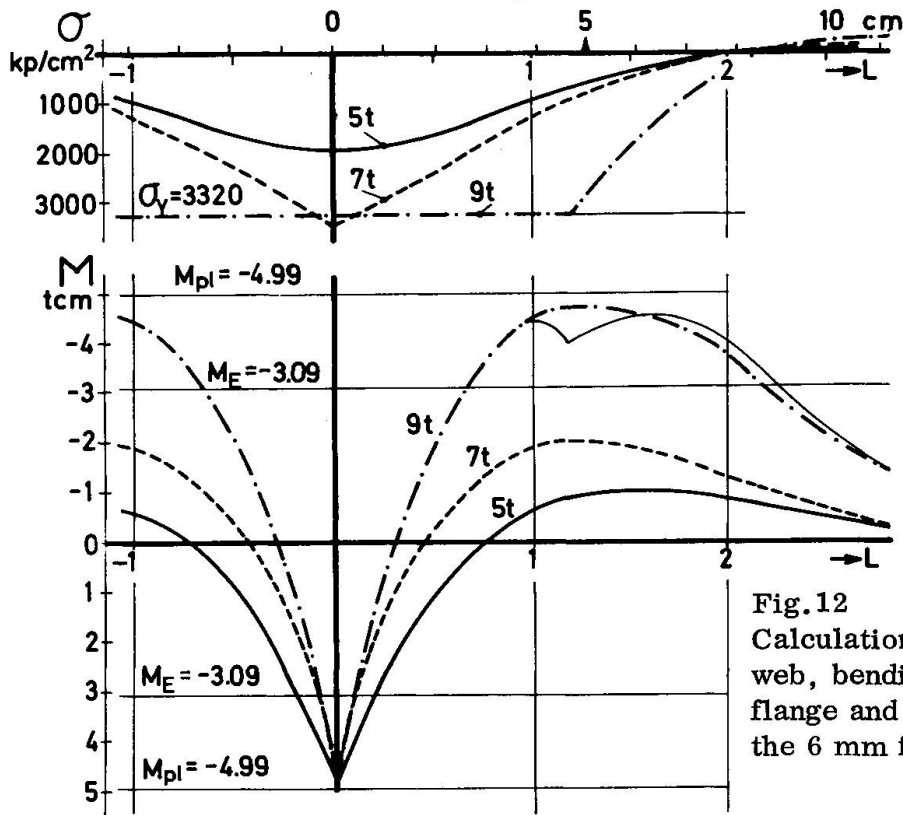


Fig.12
Calculation of stresses in the web, bending moment in the flange and crippling load for the 6 mm flange.

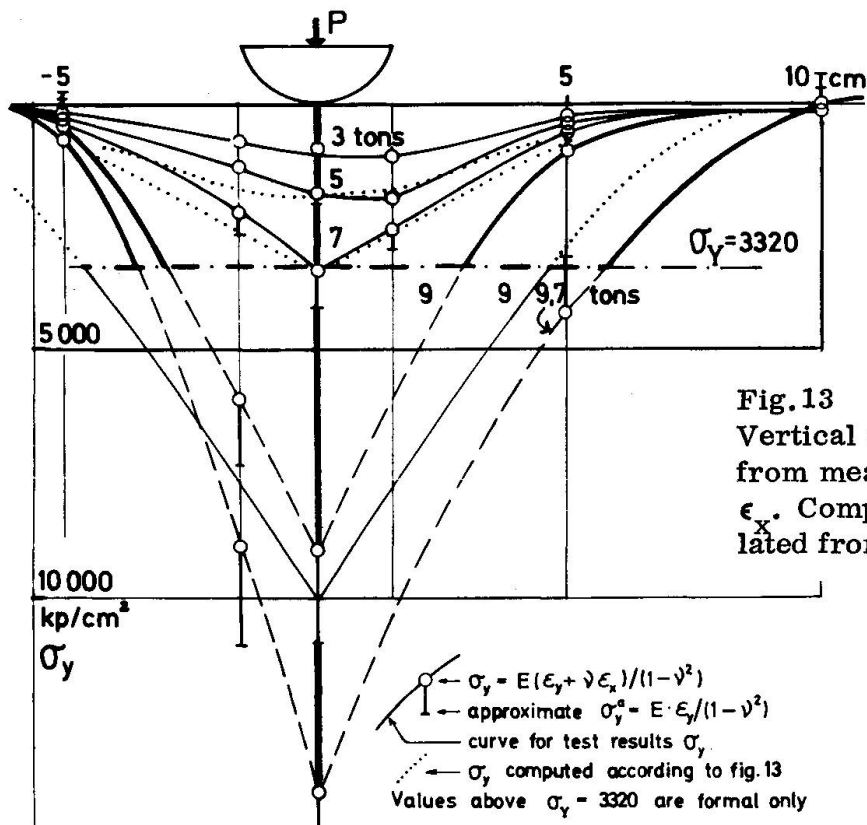


Fig.13
Vertical stresses σ_y calculated from measured strains ϵ_y and ϵ_x . Comparison with σ_y calculated from fig.12.

By a load increment from 7 to 9 tons the flange functions as two semiinfinite beams loaded with 1 ton at the ends and with the reactive pressure near the ends equal to the difference between σ_Y and the earlier existing stress, while the pressure further away is the same as for a beam on elastic springs. With dividing points situated at 4,7 cm from the point load the moment there is 2,0 tcm and the stress $\sigma = \sigma_5 + \sigma_{5-7} + \sigma_{7-9} = 800 + 200 + 2300 = 3300 \text{ kp/cm}^2$ or approximately equal to σ_Y . The assumption of a direct change at the dividing points makes a small approximation of the calculated moments near the dividing points necessary as done on fig. 12.

The moment diagram shows that the flange moment is approximately 4,7 tcm at about 4,7 cm from the point load. As the yield moment is $M_{pl} = 4,99 \text{ tcm}$ the load can only be increased somewhat over $P = 9 \text{ tons}$ before the bearing capacity fails if strain hardening is neglected. The real collapse load was 9,7 tons. On fig. 13 the vertical stresses of test B2 is shown for different load stages. Here also the calculated stresses are shown. As seen the agreement between the simplified theory and the experimental values are very good both regarding the maximum strain and the shape of the curves.

In fig. 14 results from computations of idealized I-girders with small flange thicknesses are shown. In the same diagram the buckling load from the following section B is shown. The measured test values for knife-edge load are also plotted. It is seen that for girders with flanges thinner than about $2d$ computations according to the "theory of beams on elastic foundation" limit the concentrated loads.

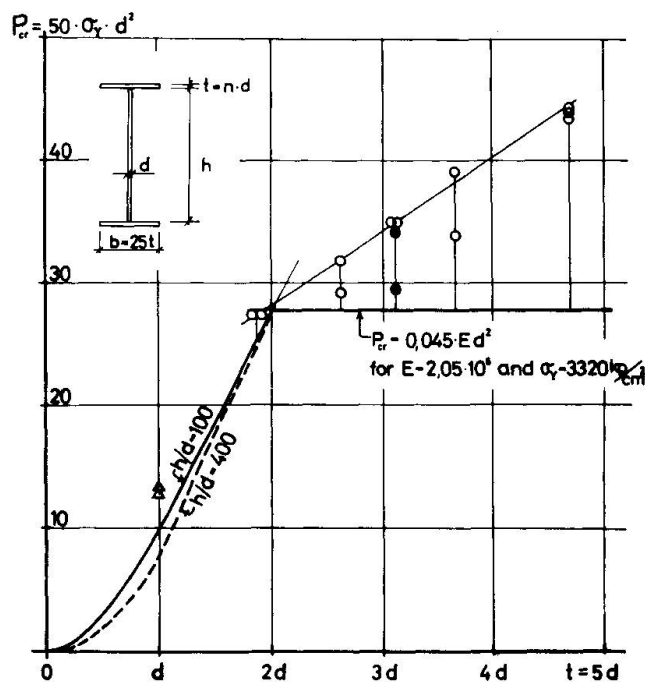


Fig. 14 b → Idealized dependence on δ_{init} of the lateral deflection and of P_{cr} .

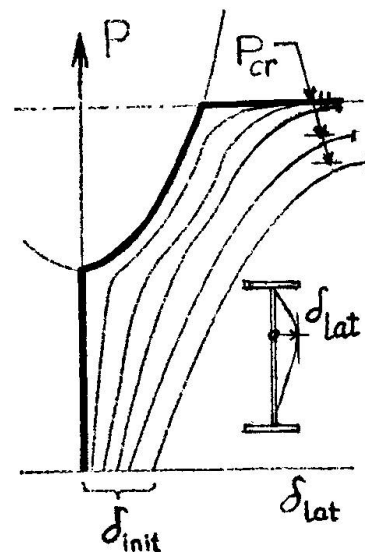


Fig. 14 $P_{cripple}$ calculated for idealized girders with $b = 25 t$ and $t = n \cdot d$. For $t \leq 2d$ the flange is calculated as a beam on elastic foundation ($h/d = 100$ and 400). For $t > 2d$

a straight line corresponding to the approximate formula $P_{cr} = 0,045 E d^2$ is shown. Values measured for knife-edge load on the test girders are marked. As further comparison (for $t = d$) the values measured for lipped channels and with transfer length $c/a = 0,04$ are plotted from [15].

In case of great flange thickness the flanges computationally are strong enough to distribute the stresses from the point load against the web without giving stresses far out of the elastic range as in the case of 6 mm flange thickness. The distribution length is so great that buckling over a greater part of the web height is actual, c.f. the following section B.

B. Web buckling

Some earlier theoretic derivations [15] [16] of the buckling loads of ideal plates supported along all edges may be summarized as follows

$$[15] \dots P_{total} = p \cdot c = K_Z \frac{c \pi^2 D}{a^2} \text{ and } [16] \dots P_{total} = K_R \frac{a \pi^2 D}{h^2}$$

The formulas can of course be used to compute a new coefficient K such that $P_{total} = K \frac{\pi^2 D}{h}$. Introducing the plate stiffness $D = \frac{Ed^3}{12(1-\nu^2)}$ one obtains

$$P_{total} = K \frac{\pi^2 Ed^3}{12(1-\nu^2)h} = k \cdot E \frac{d^2}{h/d} \text{ where } k = \alpha K_R \frac{\pi^2}{12(1-\nu^2)}$$

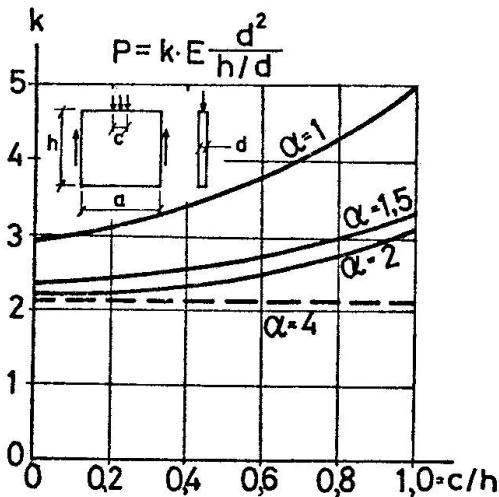


Fig. 15
Variation on buckling coefficient k with apex ratio $\alpha = a/h$ and loading length ratio c/h for a plate.

In fig. 15 the coefficient k is given as a function of α and distribution length c/h . The last ratio has been chosen instead of the more traditional c/a , as the intension is to illustrate girder behaviour and not plate action. For those α -values where both coefficients K_Z and K_R are given in [15] and [16] respectively, the values of k are the same independent of the initializing ones.

On the figure K_R has been used for $\alpha = 1$ and 1,5 and 2, while for $\alpha = 4$ there are only the clearly approximate values of K_Z given and there the mean values of K_Z for $c/h = 0,06$ and $0,20$ have been used.

Naturally the buckling load of a plate is increased in case it is supplied with flanges to form an I-section. In [16] for a plate element with $\alpha = 1$ and $c/h = 0,2$ the values of the buckling coefficient are $7,75/3,48 = 2,22$ to $8,13/3,48 = 2,34$ times greater in case of flanges with thickness ratios $t/d = 2$ to 5 than for the case of no flanges.

From the tests it can be concluded that even if the lateral web deflection may develop in a shape as assumed in [15] and [16] the final bearing capacity is limited by the great web deformations in a region of the upper part of the web directly under the point load.

From an earlier test series [9] it is clear that the expression for the buckling load $P = k \cdot E \frac{d^2}{h/d}$ is not appropriate to describe the final bearing capacity.

Fig. 16 shows the results of the tests done for different heights h , but with constant web thickness d and thus varying h/d . P is there approximately independent of the variation of d/h . Thus a better formula for collapse load would be $P = k_u Ed^2$.

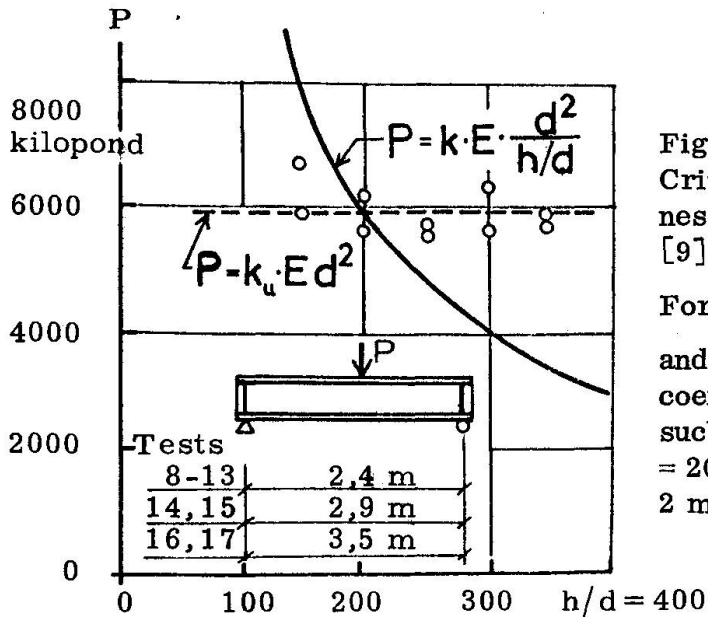


Fig. 16
Crippling loads for different web slenderness ratios. The test values are from ref. [9].

For comparison the curves $P = k \cdot E \frac{d^2}{h/d}$ and $P = k_u \cdot E \cdot d^2$ are shown. Here the coefficients k and k_u are determined to such values which give coincidence for $h/d = 200$. (The web thickness was nominally 2 mm but the real thickness was greater.)

Applied to the test values the considerations in the preceding sections show that in case of strong flanges, the local compressive stresses in the web are not decisive. The flange distributes the load over such a great length in relation to the height of the girder that buckling ought to dominate, the combination probably resulting in crippling. For example in case of a flange thickness of 15 mm one obtains *) respectively $2 L_0/h = 2 \cdot 9,35/70 = 0,27$ or $2 L_T/h = 2 \cdot 30,6/70 = 0,88$ from Table 3.

a. - If the diagram in fig.15 is used **) with a correction for the flange thickness according to [16] one would obtain

$$P = 2,34 \cdot 2,1 \cdot 2,1 \cdot 10^6 \cdot \frac{0,326^2}{70/0,326} = 5230 \text{ kp} = 5,23 \text{ tons}$$

As the measured greatest loads varied from 15,4 to 15,8 the agreement is not good partially due to the restraint caused by the upper flange. (Correcting for the restraint with regard to the coefficient in the following section one obtains $5,23 \cdot 5,32/1,88 = 14,8$ tons.)

b. - The traditional simplified theory of buckling under a point load on the flange assumes a distribution on a length equal to the height of the girder (corresponding to a distribution at an angle of 45° down to the axis of the center of gravity of the girder). Making the simplifying assumptions that the web of the test girder is fully restrained by the upper and hinged at the lower flange, and assuming linear variation from the loaded to the unloaded flange, one obtains

$$P = 5,32 \cdot \frac{\pi^2 EI}{(1-\nu^2)h^2} = 4,77 \cdot E \frac{d^2}{h/d}, \text{ as } I = \frac{h \cdot d^3}{12}$$

*)

It may be observed that the expression L/h corresponds to the flange flexibility parameter used in [16] multiplied with α^3 for the aspect ratio, that is $L/h = \sqrt[4]{\alpha^3 I/b^3 t}$ with the symbols of [16].

**)

At the calculations the value $E = 2,1 \cdot 10^6 \text{ kp/cm}^2$ generally applied in European papers has been used. The measurements shown in Table 2 gave however the value $2,05 \cdot 10^6 \text{ kp/cm}^2$.

The form of the expression is the same as above and the coefficient is corrected as to the restraint. The buckling load would be 5,07 tons, even somewhat less than the much to low value obtained above.

An increase in distribution length from h to $h + 2L$ gives better values but they are still to low. Also plate action must be considered.

c. - The empirical formula $P = k_u \cdot Ed^2$ will give with $k_u = 0,45 \cdot 10^{-4}$ the value $P = 10,0$ tons.

C. Web crippling

The shear stresses for the slender webs considered here does not correspond to a linear load distribution down to the unloaded flange, but the load transmission is concentrated to the region under the point load. This fact which is verified by the strain gage measurements means that the buckling lengths are shorter and thus the buckling loads greater.

At the same time for the real girders there were some initial deviations from planeness of the web. This means that even at the start of loading the compressive stresses act in combination with bending stress.

A treatment of the test values as to this effect is in progress.

D. The influence of A, B and C on the bearing capacity of the girder

If the bending stresses or the shearing stresses in the girder on the whole are great (but still under allowed values) and are of the same sign as the local stresses the influence of combined action reduces the capacity to support a point load somewhat, and vice versa. An earlier example is shown in fig. 8. A further test value is obtained by comparison between the tests G_u and E_u where the increase in span width from 2,4 to 9,4 meters with a corresponding increase in σ_x has reduced the capacity to carry point loads from 12,3 to 10,4 tons, e.g. a reduction of about 15 %.

Summary and Conclusion

From Part I of the article is seen, in fig. 4, that tests on shear buckling of plate girders without intermediate web stiffeners support the approximate solution of ultimate bearing capacity given by Bergman [5]. The influence of coexisting bending stresses and of initial lateral deformations is small. This is in contrast to the behaviour predicted on linear small deflection theory.

In Part II formulas for crippling load are discussed and compared to new tests. The empirical formula

$$P_{cr} \text{ tons} = 0,9 \cdot d^2_{mm} \quad \text{or} \quad P_{cr} = 0,045 \cdot Ed^2$$

gives fairly good values for the tested slenderness ratios $150 < h/d < 350$ and for web dimensions from 2 to 6 mm. This holds true for I-girders, where the web to some extent is restrained by the flange. As is seen from fig. 14 for very thin flanges, $t < 2d$ (or cold formed profiles) it is necessary to check the yield stress of the web (e.g. with

yield zones in the flange computed as for beams on elastic foundations). For thicker flanges P_{cr} increased and reached in these tests for very plane webs $P_{cr} = 0,045 \cdot Ed^2 \cdot (0,55 + 0,035 L/d)$ or, still more approximately $P_{cr} = 0,045 \cdot Ed^2 (0,55^{cr} + 0,22 t/d)$. When the webs had great initial lateral deflections P_{cr} was lower, c.f. fig.14 b, but with $0,045 \cdot Ed^2$ as lowest boundary. In some tests where the flange was thin, the load not fixed and the web thus almost hinged at the flange, there was a reduction to about 70% of the above values.

If the load was transmitted by a bar plate of the length of 30 d (or h/7) instead of by a knife edge, P_{cr} increased about 10% for thin girder flanges. This increase diminished to about 5% for the thickest flange of the tests (fig.11). When the bar was 60d long, P_{cr} was further increased some few %.

The influence of high bending and shear stresses (allowable stresses) reduced P_{cr} only about 15% compared to values at small stresses.

For repeated loading cycles to 80% of the P_{cr} for one loading only there was no failure after 100 cycles, though snap buckling took place and strains up to 3,8 ‰ were measured for pressure and bending stresses in the web.

It is intended to do further tests.

*

REFERENCES

- 1 H.Wagner : Ebene Blechwandträger mit sehr dünnen Stegblech. Zeitschrift f. Flugtechn. u. Motorluftschiffahrt, vol.20, 1929.
- 2 K.Basler - B.Thürlimann : Strength of plate girders. Proc.ASCE, ST 6 and 7, 1961.
- 3 K.C.Rockey - M.Skaloud : Influence of flange stiffeners upon the load carrying capacity of webs in shear. IABSE, New York 1968, p.429.
- 4 Th.v Kármán : The engineer grapples with non-linear problems. Bull.Am. Math. Soc. vol.46, 1940.
- 5 S.Bergman : Behaviour of buckled rectangular plates under the action of shearing forces. Theses, KTH, Stockholm 1948.
- 6 C.A.Granholm : Provnig av balkar med extremt tunt liv. (Tests on girders with extremely thin web plates). Rapport 202, Inst.f.Byggnadsteknik, CTH. Göteborg 1960-61.
- 7 C.A.Granholm : Lättbalkar (Light girders). Teknisk Tidskrift, Stockholm 1961, p.455.
- 8 Hj.Granholm : Svetsade balkkonstruktioner (Welded girders). Jernkont. Ann. 148 (1964):10. Uppsala, Sweden 1964.
- 9 A.Bergfelt - J.Hövik : Thin-walled deep plate girders under static loads. IABSE 1968, New York, p.465.
- 10 A.Bergfelt - J.Hövik : Shear failure and local web crippling in thin-walled plate girders, Experiments 1966-69. CTH, Stål- och Träbyggnad, Int.skr. S70:11b, Göteborg 1970.
- 11 F.Nishino - T.Okumura : Experimental investigation on strength of plate girders in shear. IABSE, New York 1968, p.451.
- 12 Ph.Carskaddan : Shear buckling of unstiffened hybrid beams. Proc.ASCE, ST 8, Aug.1968.

- 13 A. Ostapenko - B. Yen - L. Beedle : Research on plate girders at Lehigh University. IABSE, New York 1968, p. 441.
- 14 Klöppel - Lie : Beulung des rechteckigen, allseitig belasteten und einspannungsfrei gelagerten Bleches. VDI-Zeitschrift, Bd 86, H5/6, 1942.
- 15 L. Zetlin : Elastic instability of flat plates subjected to partial edge loads. Proc. ASCE, Vol. 8, Paper 795, 1955.
- 16 D. K. Bagchi - K. C. Rockey : A note on the buckling of a plate girder web due to partial edge loadings. IABSE, New York 1968, p. 489.
- 17 Ch. Schilling : Web crippling tests on hybrid beams. Proc. ASCE, ST1, Feb. 1967.
- 18 A. W. Hendry : The stress distribution in a simply supported beam of I-section carrying a central concentrated load. Proc. Soc. for Experimental Stress Analysis, Vol. VII No 2, 1949, pp 91-102.

SUMMARY

From Part I of the paper it is seen that tests to failure on shear buckling of plate girders with thin webs without intermediate web stiffeners, fig. 4, support the approximate solution of ultimate bearing capacity already given by Bergman (5).

The tests of Part II illustrate that for these girders the failure in web crippling under concentrated loads is limited by bending and compression stresses in the web and in the flange up to a flange thickness of about twice the web thickness. For thicker flanges the web buckling dominates and the load increases slightly in proportion to flange thickness, fig. 11 and fig. 14.

RESUME

Les essais de la première partie de l'article, fig. 4, confirment les résultats de la solution approximative de Bergman (5) concernant la résistance au cisaillement.

Dans la seconde partie il est démontré que la résistance à la rupture de l'âme sous charges concentrées est limitée par les tensions de compression et de flexion dans l'âme et dans les semelles pour une épaisseur de la semelle qui est le double de l'épaisseur de l'âme (voir fig. 14). Pour des semelles plus épaisses le voilement prédomine et la charge n'augmente que faiblement pour des épaisseurs élevées de la semelle, fig 11.

ZUSAMMENFASSUNG

Im ersten Teil dieses Aufsatzes wird gezeigt, dass Versuche über die Beulung durch Querkraft, Bild 4, für Blechträger mit dünnen Stegen die approximative Lösung über das Bruchverhalten bestätigen, die schon von Bergman (5) gegeben wurde.

Die Versuche im zweiten Teil zeigen, dass das Bruchverhalten des Steges unter Punktlasten durch die Biege- und Druckspannungen im Steg und im Flansch bei einer Flanschdicke von ungefähr doppelter Stegdicke begrenzt wird. (Bild 14). Für dickere Flanschen überwiegt die Beulung, und die Last nimmt nur wenig mit erhöhten Flanschdicken zu (Bild 11).

Leere Seite
Blank page
Page vide